Infectious Disease Modelling 10 (2025) 758–774

Contents lists available at ScienceDirect

Infectious Disease Modelling

journal homepage: www.keaipublishing.com/idm

The interaction between population age structure and policy interventions on the spread of COVID-19

Hao Yin [a, b, c, *], Zhu Liu [a], Daniel M. Kammen [d, e, f]

[a] Ministry of Education Key Laboratory for Earth System Modeling, Department of Earth System Science, Tsinghua University, Beijing, 100084, China
[b] Department of Economics, University of Southern California, CA, 90089, USA
[c] School of Population and Public Health, University of British Columbia, Vancouver, BC, V6T 1Z3, Canada
[d] Energy and Resources Group, University of California, Berkeley, CA, 94720, USA
[e] Goldman School of Public Policy, University of California, Berkeley, CA, 94720, USA
[f] Renewable and Appropriate Energy Laboratory, University of California, Berkeley, CA, 94720, USA

ARTICLE INFO

Article history:
Received 22 June 2024
Received in revised form 11 November 2024
Accepted 9 March 2025
Available online 10 March 2025
Handling Editor: Dr Yijun Lou

ABSTRACT

COVID-19 has triggered an unprecedented public health crisis and a global economic shock. As countries and cities have transitioned away from strict pandemic restrictions, the most effective reopening strategies may vary significantly based on their demographic characteristics and social contact patterns. In this study, we employed an extended age-specific compartment model that incorporates population mobility to investigate the interaction between population age structure and various containment interventions in New York, Los Angeles, Daegu, and Nairobi – four cities with distinct age distributions that served as local epicenters of the epidemic from January 2020 to March 2021. Our results demonstrated that individual social distancing or quarantine strategies alone cannot effectively curb the spread of infection over a one-year period. However, a combined strategy, including school closure, 50 % working from home, 50 % reduction in other mobility, 10 % quarantine rate, and city lockdown interventions, can effectively suppress the infection. Furthermore, our findings revealed that social-distancing policies exhibit strong age-specific effects, and age-targeted interventions can yield significant spillover benefits. Specifically, reducing contact rates among the population under 20 can prevent 14 %, 18 %, 56 %, and 99 % of infections across all age groups in New York, Los Angeles, Daegu, and Nairobi, respectively, surpassing the effectiveness of policies exclusively targeting adults over 60 years old. In particular, to protect the elderly, it is essential to reduce contacts between the younger population and people of all age groups, especially those over 60 years old. While an older population structure may escalate fatality risk, it might also decrease infection risk. Moreover, a higher basic reproduction number amplifies the impact of an older population structure on the fatality risk of the elderly. The considerable variations in susceptibility, severity, and mobility across age groups underscore the need for targeted interventions to effectively control the spread of COVID-19 and mitigate risks in future pandemics.

* Corresponding author. Ministry of Education Key Laboratory for Earth System Modeling, Department of Earth System Science, Tsinghua University, Beijing, 100084, China.
E-mail addresses: yinhao@usc.edu (H. Yin), zhuliu@tsinghua.edu.cn (Z. Liu), kammen@berkeley.edu (D.M. Kammen).
Peer review under the responsibility of KeAi Communications Co., Ltd.

https://doi.org/10.1016/j.idm.2025.03.003

1. Introduction

The outbreak of COVID-19 triggered diverse and uncoordinated responses from countries across the world. As of July 2021, some countries managed to flatten the "infection curve" and cautiously began reopening their economies (Chang et al., 2022; Ryckman et al., 2021), while others faced uncertainties and risks of a rebound in infections during the post-pandemic era. Critical lessons for how the age structure of population affects the spread of infections, as well as the need to guard against surging infections demand access to models that can be ground-truthed by comparing model results in diverse urban settings for both COVID-19 infections and future pandemics.

For the most hard-hit countries, such as the US, Italy and Spain, a significant portion of the population consists of older individuals who face considerably higher risks of hospitalization and fatality. This is primarily attributed to changes in their immune systems and the impact of preexisting health conditions that tend to accumulate with age over time (Dowd et al., 2020; Verity et al., 2020a). Numerous studies have indicated that COVID-19 is particularly linked to the ageing population, making it an emergent disease of ageing (Banerjee et al., 2020; Santesmasses et al., 2020).

Senior population tends to develop severe conditions which requires more health care resources and medication (Farrell et al., 2020). Therefore, the high proportion of the old population might require much more resources in healthcare services and medical resources, which places a substantial burden on the health care infrastructure of many ageing countries. The significant differences in demographic characteristics of COVID-19 susceptibility and severity calls for targeted interventions to suppress the surge of the epidemic. Studies have emphasized the importance of incorporating demographic information in curbing the spread of the epidemic (Dowd et al., 2020). Important and critically needed modeling studies have explored the effects of different interventions, such as social distancing, school closing and city-lockdown policies (Bayham & Fenichel, 2020; Ferguson et al., 2020; Prem et al., 2020a; Tian et al., 2020; Wu et al., 2020). Social distancing has been recognized as one of the most effective mitigation strategies (Leung et al., 2020; Vahia et al., 2020). The effects of social distancing have been estimated using compartment model (Prem et al., 2020a), branching process model (Hellewell et al., 2020) and reduced form econometric model (Hsiang et al., 2020). While some models have explored age-specific effects, they did not incorporate population movement. An important study by the Imperial College COVID-19 Response Team explored the impacts of public health interventions in 11 European countries (Flaxman et al., 2020). Most recent studies have simulated the spread of COVID-19 among different age groups of population at national (Chang et al., 2020), regional (Verity et al., 2020) and community levels (Rădulescu et al., 2020). Some studies also investigated the effects of various interventions strategies, vaccination policy and population behavior on the spread of infection (Chang et al., 2020; Leung et al., 2021; López & Rodó, 2020). While existing literature has explored the age-specific effects of social distancing measures, there remains limited understanding of how population age structure affects the effects of containment interventions in relation to COVID-19 transmission.

In this study, we selected four representative cities, namely New York, Los Angeles, Daegu, and Nairobi, which encompassed both similarities and diversities in terms of socioeconomic environment, demographics, and containment strategies. By examining individual cities with relatively homogeneous policy design, we can utilize a well-described model to assess the effectiveness of interventions.

The containment measures in the four cities and their effects varied significantly. As the world's most impacted nation, the number of infected cases in the United States (US) surged to 5 million by August 9, 2020 (Johns Hopkins University, 2020). New York, the most populous US metropolitan area, was once the epicenter and is now beginning to recover the economy. By contrast, Los Angeles, had a total number of infected cases accounting for fewer than 10 % of that in New York but became the new epicenter in December 2020 (Luke and Rong-Gong, 2020). Many factors influenced such differences. The effectiveness of an intervention policy heavily depends on whether the policy is instructive for the public and if the population behaved accordingly. The rapid rise of infections in Los Angeles might be largely due to the reopening policy in May 2020 which resulted in higher a social mixing rate. Explanations for the rapid increase in the spread of COVID-19 have been discussed (Boccia et al., 2020; Dyer, 2020). Compared with the containment strategy in the US overall, South Korea implemented a relatively faster and more effective testing regime, contact-tracing, and quarantining of infected cases without fiercely reducing the daily mobility (BBC, 2020a). Detailed online instruction and clarification of requirements for isolation were widely disseminated online (Ministry of Health and Welfare, 2020). Nairobi, as the capital city of Kenya, has a relatively younger population than the other three cities (BBC, 2020b). Kenya also took a fast response since the first case was detected (BBC, 2020b). However, recent reopening policy in Nairobi induced growing infected cases across the country (Mersie & Mohammed, 2020). Overall, the four cities implemented measures of social distancing, travel restriction, school closure and personal hygiene. While South Korea and Kenya required people to wear face masks at the beginning of the outbreak, the US did not encourage people to wear face masks/face covering until April 3, 2020 (Centers for Disease Control and Prevention, 2020a). In addition, the quarantine policy in the US was not as strict as the one in South Korea and Kenya (BBC, 2020a; Mathieu et al., 2020).

In addition to the policy responses for the general population, some policies also targeted the older population as they face higher risks than younger people. For instance, Los Angeles required peopled aged 65 and older to only leave home for essential activities (County of Los Angeles Public Health, 2020). While the US Centers for Disease Control and Prevention recommended specific measures for older adults (Centers for Disease Control and Prevention, 2020b), the growing infected cases among younger people also endangered the elderly. The difference in the interaction of these non-pharmaceutical interventions and age structures of population might deviate the transmission rate of COVID-19.

To address the above research gaps and policy challenge, we developed an age-specific and population-dynamic SEIR-HQD (susceptible-exposed-infected-recovered-hospitalized-quarantined-dead) model and applied it to four cities to analyze the age-specific effects of non-pharmaceutical interventions. Additionally, we incorporated population mobility to explore its impact on infection spread. By utilizing counterfactual population age structure, we assessed its influence on the effectiveness of containment responses. The findings of this study have important implications for designing targeted strategies that prioritize specific age groups to protect public health and support economic recovery for managing future public health emergencies.

2. Materials and methods

In this study, our primary focus is on four representative cities: New York, Los Angeles, Daegu, and Nairobi. These cities were selected to capture a diverse range of socioeconomic environments, demographics, and containment strategies. Both New York and Los Angeles are global cities in the United States, sharing similarities in their economic conditions and population age structures. Both cities attract large populations and international travelers, which poses challenges in dealing with imported infections. In contrast, Daegu and Nairobi exhibit distinct economic conditions and varying population age structures. Daegu is the largest inland city in South Korea, while Nairobi serves as the capital and largest city in Kenya. By choosing cities with similar and distinct socioeconomic and demographic conditions, we aim to conduct comparative analyses and draw meaningful insights. This approach allows us to explore how various containment strategies interact with the unique characteristics of each city and how they impact the spread of COVID-19. Overall, the selection of these four representative cities enriches the robustness and generalizability of our findings, enabling us to offer valuable policy recommendations that can be adapted to different urban settings around the world.

The overall methodology framework can be summarized as follows.

1) Analyzing time-series reproduction number and age-specific transmission rates in four cities.
2) Creating counterfactual transmission matrices based on social mixing information for different non-pharmaceutical interventions.
3) Simulating age-specific effects of eight scenarios over a one-year period, including school closure, 50 % and 80 % working from home, 50 % and 80 % reduction in other mobility, 10 % quarantine rate, city lockdown and a combined strategy of school closure, 50 % working from home, 50 % reduction in other mobility and 10 % quarantine rate and city lockdown interventions.
4) Investigating the effects of implementing all policy responses one week earlier to inform response timing and prevent potential infection waves.
5) Assessing age-specific risks of lifting restrictions on domestic and international travel for four cities.
6) Testing the influence of population age structure on the effectiveness of containment responses by employing counterfactual population age distributions of Los Angeles, Daegu, and Nairobi in the context of New York.

This framework allows for a comprehensive evaluation of the interaction between population age distribution and containment interventions in relation to COVID-19 transmission in different cities. As the study was initially drafted in March 2021, it is important to note that there have been subsequent policy changes in response to the evolving pandemic situation. However, it is worth mentioning that the methodology used in this study remains applicable and adaptable to any stage of the pandemic.

2.1. Traveler data and infected incidence

We stratified each population into 9 age groups by a 10-year band, with the last age group set as those 80 years and older. We simulated both natural population dynamics (birth and death rates) and population movement due to inbound and outbound travelers in each city. In this study, we collected inbound international inbound and outbound traveler statistical data from multiple global and local statistical sources (Korea Tourism Organization, 2020; LA County, 2018; National Travel and Tourism Office, 2020; NBC Los Angeles, 2019; NY City Tourism and Conventions, 2020; Our World in Data, 2020; The World Bank, 2020; Trading Economics, 2020). For domestic travel data, we obtained information for each city as follows: New York City data from the NYC Annual Report 2019 (Office of the New York State Comptroller, 2021), Los Angeles data from the LA County Annual Report 2017 (LA County, 2018) and an NBC Los Angeles news article (NBC Los Angeles, 2019), Daegu data from the Korea Tourism Survey (Korea Tourism Organization, 2020), and Nairobi data from Trading Economics on Kenya Tourist Arrivals (Trading Economics, 2020). For Nairobi, since city-level data on domestic visitors was unavailable, we assumed the number of inbound travelers from other cities to be proportional to Nairobi's population. We first estimated the number of travelers from other regions of the country by multiplying the total domestic travelers by the proportion of the population outside Nairobi relative to the national population. Next, we assumed that the number of these travelers visiting Nairobi would be proportional to city's share of the national population. We estimated the daily average of domestic inbound visitors to Nairobi at the city level using the following calculation (Eq. (1)):

$$d.IT_{nairobi} = \frac{T_{\boldsymbol{ke}nya,\boldsymbol{d}}}{365} \times \frac{Pop_{Kenya} - Pop_{Nairobi}}{Pop_{Kenya}} \times \frac{Pop_{Nairobi}}{Pop_{Kenya}} \quad (1)$$

where $d.IT_{nairobi}$ represents the average daily domestic inbound travelers to Nairobi,
$T_{kenya,d}$ is the total annual domestic travelers in Kenya,
365 is the average number of days in a year;
Pop_{Kenya} is the total population of Kenya;
$Pop_{Nairobi}$ is the population of Nairobi.

City-level data on the number of outbound travelers was unavailable. Therefore, we estimated the number of outbound travelers from each city by applying the total annual national domestic travelers and scaling it by the ratio of the city's population to the national population. This was calculated using the following equation (Eq. (2)):

$$d.ET_{city} = \frac{T_{\boldsymbol{ctr},\boldsymbol{d}}}{365} \times \frac{Pop_{city}}{Pop_{ctr}} \quad (2)$$

Where $d.ET_{city}$ represents the daily average of outbound travelers from each city,
$T_{\boldsymbol{ctr},\boldsymbol{d}}$ is the total annual domestic travelers within the country,
Pop_{city} and Pop_{ctr} are the populations of the city and the country, respectively.

The estimates of daily average inbound and outbound travelers from international and domestic destination before the outbreak of COVID-19 are summarized in Table 1.

The domestic and international incidences of COVID-19 were estimated using daily infected cases divided by the total number of travelers (Eqs. (3) and (4)):

$$\mathrm{i}.\theta_t = \frac{i.I_t}{i.T} \quad (3)$$

$$\mathrm{i}.\theta_t = \frac{i.I_t}{i.T} \quad (4)$$

where $\mathrm{i}.\theta_t$ and $\mathrm{d}.\theta_t$ are global and domestic incidence of COVID-19 infection in day t, and $i.I_t$ is global daily infected cases in day t, and $d.I_t$ is domestic daily infected cases in day t.

In this study, age-specific incidence rates for travelers were essential for our mathematical model. However, as direct age-specific incidence data for travelers was unavailable, we adjusted the overall incidence rates to estimate age-specific rates using the age distribution of both global tourists and the national population. Specifically, age-specific infection incidence rates were derived by multiplying the total incidence rate by the proportion of each age group within the population.

2.2. Population mobility

We retrieved population mobility data from Google Covid-19 community mobility reports from February 2020 to March 2021 (Google. Covid, 2020). Fig. 1 shows the change of mobility in each city since the outbreak of COVID-19. The mobility in working, other activities and school substantially dropped between march and mid-April 2020 in New York, Los Angeles and Nairobi. By contrast, Daegu did not show as much reduction in terms of any category of mobility comparing with the other three cities. The average mobility increased after mid-April 2020 due to the opening up policy in the US. From the mobility data, we can also tell that Nairobi started loosening their social distancing and working-at-home policies since April 2020. The mobility of home increased since the intervention strategies were implemented, which might indicate growing contact rates at home.

The time series of contact matrices were adjusted based on daily changes in mobility. Specifically, we used pre-pandemic mobility data as the baseline for each type of activity and calculated the relative mobility proportion during each policy intervention period. We then estimated the adjusted time-series contact matrices by multiplying the pre-pandemic contact matrices by the mobility proportion for each activity type.

Table 1
Daily import and export travelers in the four cities before the outbreak of COVID-19.

Travelers	New York	Los Angeles	Daegu	Nairobi
Domestic import	154637	116438	31085	1117
International import	13658	20548	2289	2773
Domestic export	162450	113535	31176	931
International export	13231	20125	3752	361

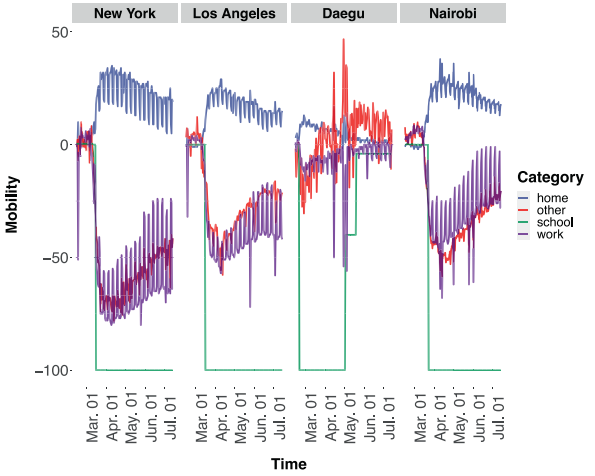

Fig. 1. Mobility change since the outbreak of COVID-19 in the four cities.

2.3. SEIR-HQD model framework

In this study, we adapted an SEIR model to an age-specific SEIR-HQD model for a period of 365 days. SEIR-HQD model considers 7 states of infection including susceptible (S), exposed (E), infectious (I) and recovered (R), hospitalized (H), quarantined (Q) and dead (D). The SEIR-HQD model incorporates the age structure, growth rates and death rates dynamics of the affected population in Daegu, New York, Los Angeles and Nairobi.

Fig. 2 summarizes the components and movement among different compartments in the SEIR-HQD model. We added the population birth and death rates into each compartment of the SEIR-HQD model. In the model, we also simulate the dynamics of population movement in each city.

2.4. Mathematical model and parameter setting

When the susceptible populations are exposed to infectious individuals, a percentage then transition into infected status at a given probability defined by an age-specific transmission rate. After the incubation period, the exposed population then become infectious, but if they are quarantined, we assume that they do not impact susceptible individuals in the next generation. For those who are infectious, given the hospitalization rate of infectious cases, we further calculate the number of people who are in need of further medical care in the hospital. Our model also simulates the quarantine of individuals and hospitalized cases are sub-states of infected cases that will not cause a secondary infection. The quarantine individuals might also become hospitalized.

The epidemic evolution model is described as follows (Eqs. (5)–(11)), which describes the daily change in susceptible ($\frac{dS_{i,t}}{dt}$), exposed ($\frac{dE_{i,t}}{dt}$), infected ($\frac{dI_{i,t}}{dt}$), hospitalized ($\frac{dH_{i,t}}{dt}$), dead ($\frac{dD_{i,t}}{dt}$), quarantined ($\frac{dQ_{i,t}}{dt}$) and recovered ($\frac{dR_{i,t}}{dt}$) compartments. Each equation describes the change rate of specific population in each age group. For example, the susceptible population increases

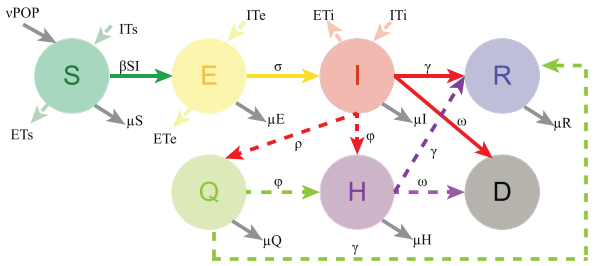

Fig. 2. Schematic framework of SEIR-HQD epidemic model. "POP" refers to the total population in each city, which is equivalent to the initial susceptible population in this context. "S" = Susceptible, refers to the susceptible population, "E" = Exposed, refers to infected but not infectious yet, "I" = Infected, refers to the population that is infected and infectious, encompassing both symptomatic and asymptomatic individuals, "R" = Recovered, refers to the population that is recovered, "Q" = Quarantined, refers to the population that is quarantined, "H" = Hospitalized, refers to individuals who are hospitalized, "D" = Dead, refers to the population that is dead. "ITs" and "ETs" refer to the imported and exported travelers who are susceptible, respectively. "ITe" and "ETe" refer to the imported and exported travelers who are exposed, respectively. "ITi" and "ETi" refer to the imported and exported travelers who are infected, respectively. ν is the daily growth rate per thousand population, μ is the daily death rate of population, βSI refers to the infection force, σ is incubation rate, γ is recover rate, ω is the death rate of infected population, φ is the hospitalization rate, ρ is quarantine rate.

due to natural population growth, and then decreases by the number of susceptible individuals transitioning into the infected compartment. Additionally, the susceptible compartment accounts for domestic and international travel by adding new inbound population and excluding those who have been exposed to infected cases. Similarly, the other compartments capture the dynamics of transitions from the preceding compartments, including imported and exported cases from domestic and international sources for the corresponding compartments.

$$\frac{dS_{i,t}}{dt} = \frac{\nu}{n}\sum_{i=1}^{n} pop_i - \frac{\boldsymbol{\beta_i}\left(\boldsymbol{I_{0,age}} - \boldsymbol{H_{0,age}} - \boldsymbol{Q_{0,age}}\right)'}{pop_i} \times S_{i,t} - \mu_i S_{i,t} + \left[i.IT_{i,t} \times \left(1 - i.\theta_{i,t}\right) + d.IT_{i,t} \times \left(1 - i.\theta_{i,t}\right) \times \right] - \frac{\left(i.ET_{i,t} + d.ET_{i,t}\right)}{pop_i} \times S_{i,t} \tag{5}$$

$$\frac{dE_{i,t}}{dt} = \frac{\boldsymbol{\beta_i}\left(\boldsymbol{I_{0,age}} - \boldsymbol{H_{0,age}} - \boldsymbol{Q_{0,age}}\right)'}{pop_i} \times S_{i,t} - \sigma E_{i,t} - \mu_i E_{i,t} + \frac{i.IT_{i,t}}{\sigma} \times i.\theta_{i,t} + \frac{d.IT_{i,t}}{\sigma} \times d.\theta_{i,t} - \frac{i.ET_{i,t} + d.ET_{i,t}}{pop_i} \times E_{i,t} \tag{6}$$

$$\frac{dI_{i,t}}{dt} = \sigma E_{i,t} - \gamma_i I_{i,t} - \mu_i I_{i,t} - \omega_i I_{i,t} + i.IT_{i,t} \times i.\theta_{i,t} + d.IT_{i,t} \times d.\theta_{i,t} - \frac{i.ET_{i,t} + d.ET_{i,t}}{pop_i} \times E_{i,t} \tag{7}$$

$$\frac{dH_{i,t}}{dt} = \varphi_{i,t}\left(I_{i,t} - H_{i,t}\right) - \omega_i H_{i,t} - \gamma_i H_{i,t} - \mu_i H_{i,t} \tag{8}$$

$$\frac{dD_{i,t}}{dt} = \omega_i I_{i,t} \tag{9}$$

$$\frac{dQ_{i,t}}{dt} = \rho\left(I_{i,t} - Q_{i,t} - H_{i,t}\right) - \varphi_i Q_{i,t} - \gamma_i Q_{i,t} - \omega_i Q_{i,t} - \mu_i Q_{i,t} \tag{10}$$

$$\frac{dR_{i,t}}{dt} = \gamma_{i,t} I_{i,t} - \mu_i R_{i,t} \tag{11}$$

where $S_{i,t}$ is the susceptible population in age group i on day t,

$\boldsymbol{\beta_i}$ is a vector of transmission rates between susceptible individuals at age group i and infected individuals at all age groups estimated using Eqs. (12)–(15).

$\boldsymbol{I_{0,age}}$, $\boldsymbol{H_{0,age}}$, and $\boldsymbol{Q_{0,age}}$ are vectors of initial infected, hospitalized and quarantined cases across all age groups,

ν_t is the growth rate per thousand population on day t,

$\mu_{i,t}$ is the all-cause death rate of population in age group i on day t,

$i.IT_{i,t}$ and $d.IT_{i,t}$ are the international and domestic imported travelers,

$i.ET_{i,t}$ and $d.ET_{i,t}$ are the international and domestic exported travelers,

$i.\theta_{i,t}$ and $d.\theta_{i,t}$ are the incidence of infected cases in the international and domestic travelers, respectively,

n is the number of age groups, pop_i is the number of population in age group i,

$I_{i,t}$ is the infected people in age group i,

$E_{i,t}$ is the exposed population in age group i,

σ is the daily probability of an exposed individual becoming infectious, which equals to $1 - \exp\left(-\frac{1}{\mathrm{d}_{inc}}\right)$, d_{inc} refers to duration of average incubation time,

ρ is quarantine rate of exposed individuals,

$\gamma_{i,t}$ is the probability of an infected individual that recovers during the infectious duration d_{inf}, so that $\gamma_{i,t} = 1 - \exp\left(-\frac{1}{\mathrm{d}_{inf}}\right)$,

$\varphi_{i,t}$ is the hospitalization rate in age group i,

$\omega_{i,t}$ is the fatality rate of infected individuals,

$Q_{i,t}$ is the number of individuals that are quarantined,

$R_{i,t}$ is the number of infected individuals who have recovered.

The parameters involved in the model are obtained from literature and are presented in Table 2.

2.5. R_t estimation

To simulate the spread of COVID-19 under different policy packages, we estimated the location-specific reproduction number, $\mathrm{R_t}$, using serial interval data and incidence rates over time in the four cities. $\mathrm{R_t}$ represents the average number of secondary cases generated by each infected individual at a certain time (Prem et al., 2017). The serial interval data used in our study was obtained from Du et al. (2020). We employed Bayesian statistical inference and assumed a gamma prior

Table 2
Parameters in the age-specific SEIR-HQD model.

Parameters	Value	Reference
Basic reproduction number R_0	Varies by city, see Appendix 1.	Estimated in this study
Transmission rate	Varies by age, see Appendix 1.	Estimated in this study
Average incubation period, d_{inc}	5.8 days (4.8–6.8)	Backer et al., (2020)
Average duration of infection, d_{inf}	7–11 days (assume growing by age)	Cao (2020) and (Bi et al., 2020)
Initial number of infected, I_0	2 cases per million in four cities	Assumed in the study (Hellewell et al., 2020; Prem et al., 2020b; Tian et al., 2020)
Initial number of hospitalized, H_0	0 case	Assumed in the study (Hellewell et al., 2020; Prem et al., 2020b; Tian et al., 2020)
Initial number of quarantined, Q_0	0 case	Assumed in the study (Hellewell et al., 2020; Prem et al., 2020b; Tian et al., 2020)
Hospitalization rate, $\varphi_{i,t}$	Varies by age, see Appendix 1	Ferguson et al., (2020) and Verity et al., (2020)
Quarantine rate, ρ	0 %–10 %	Assumed in the study
Fatality rate, $\omega_{i,t}$	Varies by age, see Appendix 1.	Verity et al., (2020)

distribution for the serial interval within our transmission estimation framework. After a burn-in period of 1000 iterations, we conducted 15,000 additional iterations using Markov Chain Monte Carlo simulation. We sampled every 100th step within a 7-day evaluation window and generated serial interval estimates for a one-year period since the beginning of the outbreak in each city.

As the outbreak dates differed among the four cities, the simulation periods also varied. Specifically, the simulation periods for New York, Los Angeles, Daegu, and Nairobi were from March 2nd, 2020, to March 2nd, 2021; January 26th, 2020, to January 26th, 2021; January 20th, 2020, to January 20th, 2021; and March 13th, 2020, to March 13th, 2021, respectively.

R_t is estimated using Wallinga and Teunis approach (Wallinga & Teunis, 2004). To determine the R_0 in each city, we calculate the average value of R_t over the first 30 days since the outbreak began. The estimation of R_0 was performed using the EpiEstim package in R version 3.1.2.

2.6. Age-specific transmission rates

The transmission rate varies depending on factors such as location, population mobility, and contact probability. Therefore, we calculate the transmission rate matrix based on contact matrices in different location settings. The country-level contact matrices that were developed in Prem et al. (2017) depend on the national population density (Prem et al., 2017). To more accurately reflect social interactions within each city, we adjusted the contact matrix data by factoring in population density weights specific to each city in relation to the national average (Eq. (12)). The underlying principle is that when a certain age group has a larger population, the likelihood of individuals within that group coming into contact with individuals from other age groups increases. This adjustment allows us to better capture the specific contact patterns within each city and tailor the transmission rate matrix accordingly (Eqs. (12)–(15)).

$$C_{i,j}^{pop} = C_{i,j} \times prop_i^{city} \Big/ prop_j^{country} \tag{12}$$

$$\det(\boldsymbol{C^{pop}} - \boldsymbol{\lambda E}) = 0 \tag{13}$$

$$\boldsymbol{\tau} = \frac{R_0 \times \boldsymbol{\gamma}}{max(\boldsymbol{\lambda})} \tag{14}$$

$$\boldsymbol{\beta} = \boldsymbol{\tau} \times \boldsymbol{C^{pop}} \tag{15}$$

where $C_{i,j}^{pop}$ is the contact rate in each city between susceptible individuals at age group i and infected individuals at age group j, $C_{i,j}$ is the contact rate in corresponding country between the suspects at age group i and infections at age group j, $prop_i^{city}$ and $prop_j^{country}$ is the proportion of population to the total population at age group i in each city and at age group j corresponding country, respectively.

$\boldsymbol{\lambda}$ is the vector of eigenvalues of the contact matrix $\boldsymbol{C^{pop}}$ in each city, $\boldsymbol{E}$ is a 9×9 identity matrix, $\boldsymbol{\gamma}$ is the vector of recovery rate across all age groups. $\boldsymbol{\tau}$ is the vector of transmissibility, which is defined as the transmission probability of a contact between an infectious individual with a susceptible one, R_0 is the basic reproduction rate, and $\boldsymbol{\beta}$ is the transmission rate matrix among individuals across 9 age groups. The transmission rate represents the rate at which infectious cases generate secondary cases within an age-group population. It is the product of transmissibility and contact rates.

2.7. Scenario design for interventions and the timing of policy action

Using the SEIR-HQD model, we conducted three sets of simulations: 1) the age-specific effects of policy interventions, 2) the impact of age-targeted policy interventions, and 3) the effectiveness of policy actions at different time points since the diagnosis of the first case.

For the age-specific effects, we designed **eight** scenarios that tested different levels of school closure, working from home, reduction in other mobility, quarantine rate, and city lockdown (Table 3). The city lockdown intervention refers to both in-bound and outbound international travelers and domestic travelers are prohibited to travel during the lockdown period.

In addition to counterfactual scenarios, we also reviewed the policy actions in four cities from the first case detected to July 1, 2020 (Fig. 2). The details of policy were listed in the appendix. We simulated the effects of the real policy actions as the business-as-usual scenarios in the four cities. Then we move each strategy 1 week earlier to identify the effects of early actions.

2.8. Age structure effects for each city

We simulated the effects of age structure on the spread of COVID-19 by substituting younger age structures with an older one. In this study, Los Angeles, Daegu, and Nairobi had relatively younger populations, with 7 %, 5 %, and 2 % of their total populations over age 65, respectively, while New York had an older population with 9 % over age 65. By applying the other three cities' age structure to New York city, we aim to assess the effects of younger population on COVID-19 infections and deaths. The details of the age structure data from each city are described in Appendix p1.

In this simulation, we adjusted not only the age structure of the exposed population but also other related factors in our mathematical model, such as contact probability and transmission rate, to capture the broader influence of age distribution. Specifically, we adjusted New York's contact matrices to reflect the age structure of each of the other three cities. For example, to obtain contact matrices for New York using Nairobi's age structure, we multiplied New York's original contact matrices by the ratio of Nairobi's age structure to New York's. This adjusted contact matrix was then used to calculate new transmission rates in New York under a hypothetical age structure. The model then estimated infections and deaths using these adjusted transmission rates.

3. Results

3.1. R_t and age-specific transmission rates in four cities

We calculated the time-series reproduction number (R_t) for New York, Los Angeles, Daegu, and Nairobi (Fig. 1). The R_t estimates for all four cities exhibited a decreasing trend over time. R_0, the basic reproduction number assuming the entire population is susceptible, serves as a threshold, with $R_t < 1$ indicating that the epidemic is under control and will decline.

Averaging the first 30 days of R_t, we obtained the following R_0 estimates (with 95 % confidence intervals) for each city: 3.60 (3.16, 4.12) for New York, 3.19 (1.78, 5.04) for Los Angeles, 3.75 (2.66, 5.16) for Daegu, and 2.53 (1.44, 3.93) for Nairobi. In Fig. 1, we presented the reported policy interventions implemented in New York. As a result of enhanced social distancing and testing policies, the R_t in New York decreased below 1 after 50 days from the start of the outbreak. In Los Angeles, the R_t declined faster than in New York, but lifting the social distancing policy led to a rise in R_t starting from April. Daegu successfully contained the epidemic, maintaining R_t below 1 between February and May. However, when interventions were relaxed, a surge of reinfections occurred, causing R_t to increase. In Nairobi, R_t decreased rapidly from the first reported case. However, the R_t values remained higher than 1, necessitating the implementation of stricter social distancing and quarantine measures to control the epidemic.

Applying R_0 estimated in each city, we generated transmission rate matrices across 9 age groups. Besides factors like population density and social habits, the population age structure also affects transmission rates among different age groups, as depicted in Fig. 3. Younger and middle-age groups (under 60 years old) exhibit higher transmission rates due to their higher contact rates and mobility compared to older age groups (60 years and older). While some studies argue that younger populations are less infectious since they tend to have a higher chance of being asymptomatic (Prem et al., 2020a), there is

Table 3
Scenario design for age-specific effects analysis.

Scenarios id	School closure	Working from home	Reduction in other mobility	Quarantine rate	City lockdown
1	100 %	0 %	0 %	0 %	0 %
2	0 %	50 %	0 %	0 %	0 %
3	0 %	80 %	0 %	0 %	0 %
4	0 %	0 %	50 %	0 %	0 %
5	0 %	0 %	80 %	0 %	0 %
6	0 %	0 %	0 %	10 %	0 %
7	0 %	0 %	0 %	0 %	100 %
8	100 %	50 %	50 %	10 %	100 %

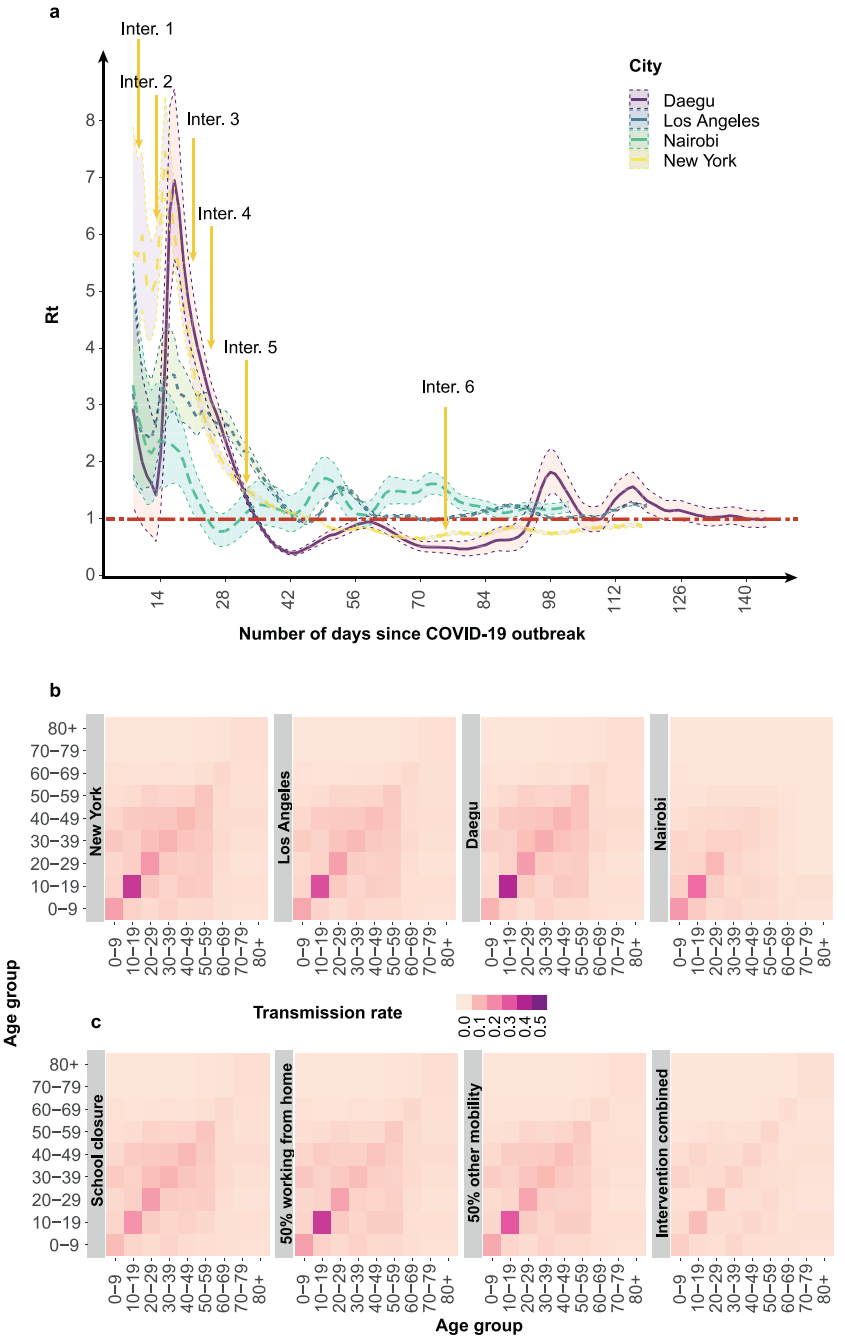

Fig. 3. R_t (a) and transmission rates (b) in New York, Los Angeles, Daegu, Nairobi and counterfactual transmission rates of different interventions (c). Fig. 3a, Inter. 1–6 are the interventions inserted at corresponding date in New York. Inter. 1 refers to interventions including city instruction for quarantine, hygiene and emergency announcement. Inter. 2 is school closing and working from home order. Inter. 3 and Inter. 4 are the enhanced public policy to increase social distancing and travel restriction. Inter. 5 required population to wear facemasks, while Inter. 6 started to implement open-up policies in New York. It shows that R_t showed decreased trends before intervention 6, however, the open-up interventions led to the rise of R_t afterwards. Fig. 3c, Intervention combined refers to intervention package including school closure, 50 % working from home, 50 % other mobility reduction.

limited information on the infectiousness of asymptomatic cases and their incidence. Thus, we assume that transmission occurs during both the presymptomatic and symptomatic stages.

Among the four cities, Daegu has the highest transmission rates, while Nairobi has the lowest. When school closure is implemented in New York, the age-specific transmission rates decrease by 50 % for the population aged 10–19. By

implementing school closure, 50 % working from home, and 50 % reduction in mobility, New York can effectively control the transmission rates to below 0.1 in all age groups.

3.2. The age-specific effects of different interventions on the spread of COVID-19

Fig. 4 presents the effects of eight intervention scenarios on the containment of infection over a year period in the four cities. The intervention scenarios include school closure, 50 % and 80 % working from home, 50 % and 80 % reduction in other mobility, 10 % quarantine rate, city lockdown and a combined strategy of school closure, 50 % working from home, 50 % reduction in other mobility and 10 % quarantine rate and city lockdown.

The effects of each intervention scenario are measured as the percentage of avoided infections compared to the scenario without interventions. School closure was found to effectively reduce transmission risks among the population under 20 years old, particularly in Daegu and Los Angeles, compared to Nairobi and New York. On the other hand, working from home mostly influenced people aged 20 and older, leading to 9 %–54 % and 15 %–61 % reductions in infections across the four cities when 50 % and 80 % of the population worked from home, respectively.

Reduction in other mobility was most effective in avoiding infections among people aged 60–80 years old in all four cities. This intervention proved particularly beneficial for cities with a higher proportion of the population aged 60 and older. Los Angeles showed the highest effectiveness, with 75 % of avoided infections when the entire population reduced 80 % of mobility for other activities, followed by New York (60 %) and Daegu (56 %), while Nairobi demonstrated 38 % of avoided infections in this scenario.

Quarantine intervention and city lockdown exhibited relatively even influence on the spread of infections across age groups. City lockdown had the most significant effect in avoiding infections in New York (over 60 % reduction) but was least effective in Nairobi.

When implemented over a one-year period, the combined strategy effectively flattened the infection curve in Los Angeles, Daegu, and Nairobi cities. However, New York might require relatively stricter social distancing measures than the other three cities to fully contain infections. These findings provide valuable insights for policymakers in designing targeted and effective interventions based on age-specific considerations for diverse urban settings.

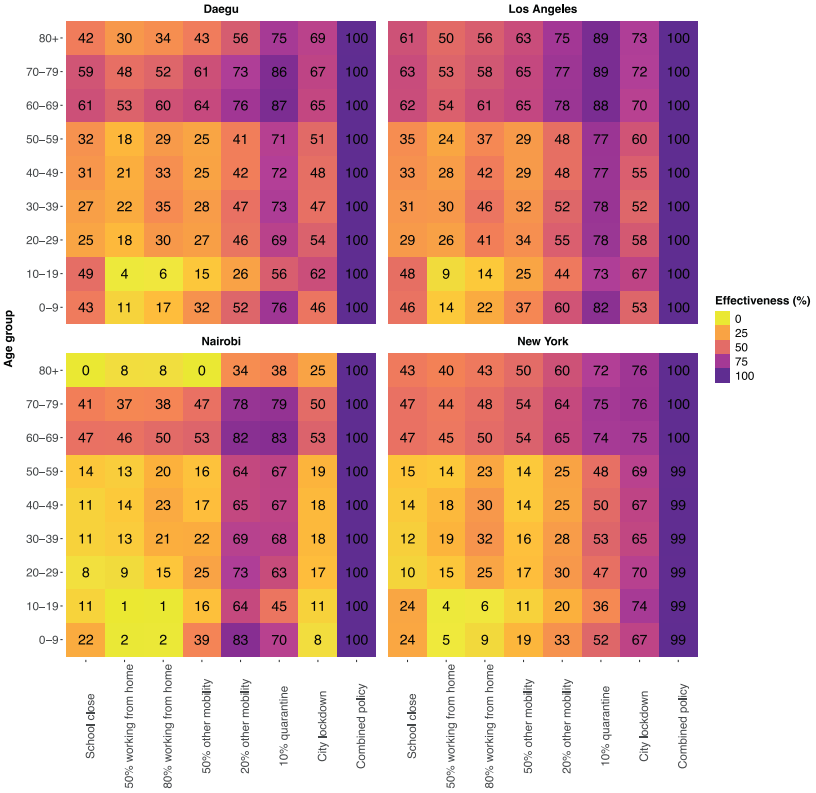

Fig. 4. The proportion of avoided infected cases to the non-intervention infection in the eight interventions targeting general population in the four cities.

3.3. Spillover effects of age-targeted regulations

Fig. 5 displays the effects of age-targeted interventions utilizing social distancing measures among specific populations. When reducing interactions among the population under 20 years old by 50 %, we observe significant spillover effects on the other age groups in the four cities.

Over the one-year period since the first case was detected in each city, implementing social distancing among the younger population can avoid close to 100 % of infected cases across all age groups in Nairobi. This highlights the importance of reducing contacts among the younger population to not only protect them but also to prevent infections in other age groups.

In contrast, reducing contacts among the population under 20 leads to a 70 % reduction in infections among people under 20 in Daegu, 33 % in Los Angeles, and 25 % in New York. Moreover, the spillover effects on other age groups are substantial, with reductions of more than 52 % in Daegu, 14 % in Los Angeles, and 10 % in New York.

However, when reducing contacts among the population older than 60 years old, the spillover effects are minimal. Strategies aimed at reducing contacts among the older population result in over 30 % avoided cases of infection for people aged 60 and older across the four cities, while the spillover effects of social distancing among the age groups younger than 60

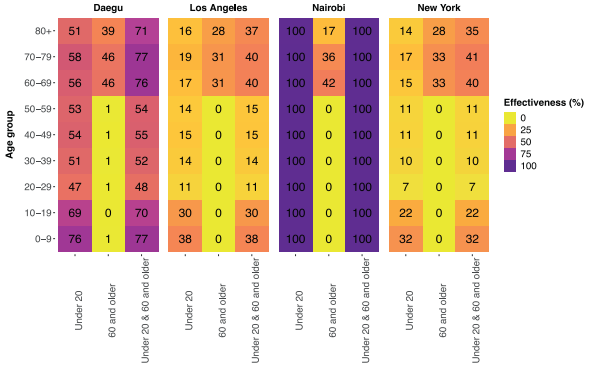

Fig. 5. Age-specific effects of regulations targeting different age groups. Each scenario is designed by reducing contacts among each other within the targeted age groups by 50 %.

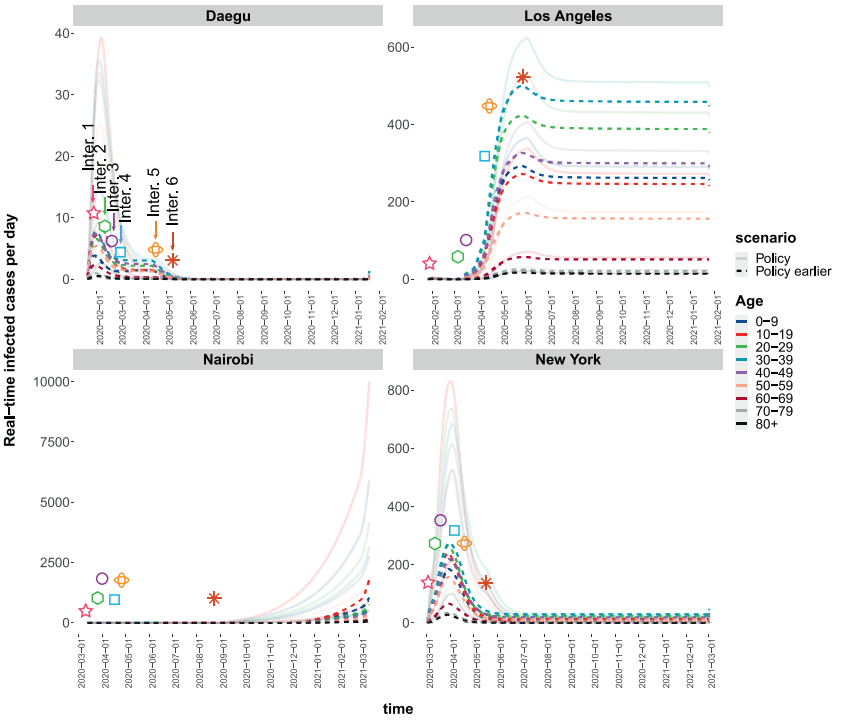

Fig. 6. Age-specific effects of 1-week earlier intervention in four cities. Details of intervention data were listed in the Appendix.

years old are less than 1 %. In comparison, social distancing among both the population under 20 and older than 60 years old slightly enhances the avoided infections across all age groups compared to social distancing among people under 20 years old.

These findings underscore the significant impact of age-targeted social distancing interventions, particularly among the younger population, in curbing the spread of infections and protecting vulnerable groups across diverse urban settings. Policymakers can use this information to design effective and targeted interventions based on the age-specific dynamics of each city.

3.4. Age-specific benefits of intervention timing

Fig. 6 illustrates the simulated COVID-19 infected cases under interventions implemented 1 week earlier compared to the timing of their actual policy interventions in the four cities. The results indicate that earlier interventions had a significant impact on reducing infections related to COVID-19 in Los Angeles, New York, Daegu, and Nairobi, avoiding 13 %, 58 %, 70 %, and 86 % of infections, respectively.

Notably, the benefits of earlier intervention were more pronounced for the population aged 50 years and older in Daegu and New York, with a 4 to 8 percentage point reduction in infections compared to the younger population. In contrast, the age-specific effects were relatively even in the other two cities. The earlier intervention strategy also proved effective in alleviating the overwhelming demand for hospital beds and other healthcare resources, easing the burden on the healthcare system. This finding highlights the importance of timely and proactive measures to control the spread of COVID-19 and reduce its impact on public health and healthcare infrastructure.

3.5. Effects of population movement

To understand the impacts of population movement on the spread of infection, we conducted a sensitivity test on the scale of population dynamics inbound and outbound from the four cities (Fig. 7). In the baseline scenario, we simulated the infected cases when regulation policies were implemented in the early stage in each city. The results demonstrated that reducing international or intercity movement led to a substantial reduction in infections in all four cities. Notably, Nairobi had more inbound travelers than outbound (Table 1), which implied that opening borders or lifting travel restrictions in Nairobi could potentially increase the risk of infection. Regarding the age-specific effects, an increase in domestic and international travelers would result in a rise of infection across all age groups with relatively even effects (Fig. 7). This finding suggests that population movement can influence the spread of infection across all age groups, highlighting the importance of considering mobility patterns in epidemic control strategies.

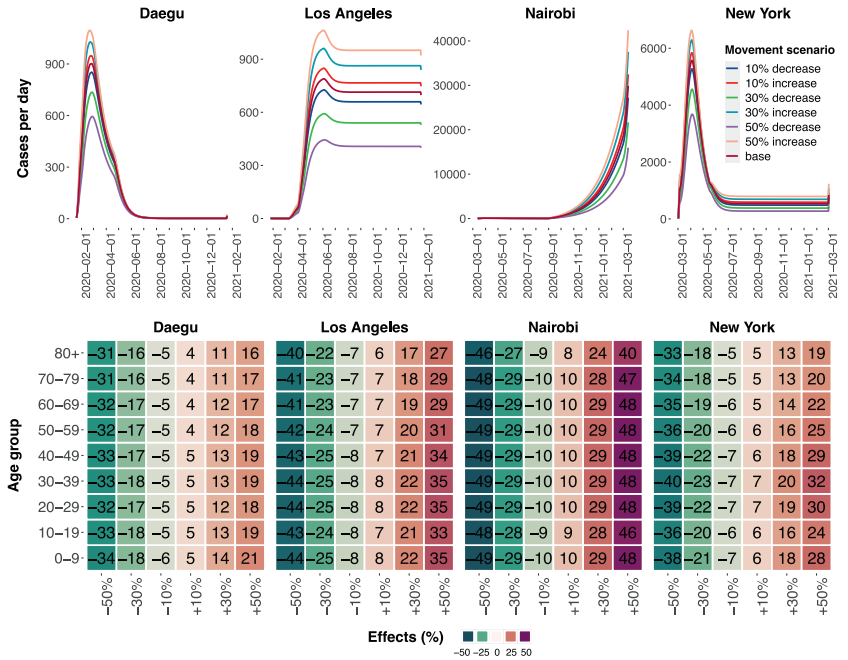

Fig. 7. The sensitivity analysis of population movement on the spread of COVID-19.

3.6. Effects of population age structure

We further investigated the influence of population age structure on the spread of COVID-19. To do this, we simulated the spread of infection in New York, where the ageing proportion (proportion of the population aged 65 and older) is 0.09, while applying the age-structure data from Los Angeles (ageing proportion: 0.07), Daegu (ageing proportion: 0.05), and Nairobi (ageing proportion: 0.02).

Fig. 8a-b illustrates the daily infection and cumulative death cases over 365 days in New York ($R_0 = 4.5$). When we replaced the age structure in New York with that from Los Angeles, Daegu, and Nairobi, the infection increased by 6.7 %, 2.2 %, and 0.4 %, respectively (Fig. 8c-d). However, adopting a younger population structure from Los Angeles, Daegu, and Nairobi resulted in avoiding 8.5 %, 15.4 %, and 42.0 % of deaths, respectively, compared to the death toll projected with the age structure in New York. These findings underscore the significant impact of population age structure on the transmission and mortality patterns of COVID-19 in different cities.

We also examined the sensitivity of the basic reproduction number (R_0) on the spread of COVID-19 concerning changes in population age structure. As expected, the infection and death cases increased with higher R_0 values (Fig. 8a-b). However, the influence of R_0 on the spread of COVID-19 in populations with different age structures remained less understood. To investigate this, we simulated the spread of infection in New York with various R_0 values, using the counterfactual age structures of Los Angeles, Daegu, and Nairobi.

If New York had a younger population structure similar to Nairobi, it would avoid 31.7 %, 38.2 %, 42.0 %, and 43.8 % of deaths for R_0 values of 2.5, 3.5, 4.5, and 5.5, respectively. This indicates that an older age structure's impact on the spread of COVID-19 is amplified with higher R_0 values. Conversely, if New York adopted the age structure of Nairobi, the infection cases would increase by −0.3 %, −0.3 %, 0.4 %, and 1.7 %, respectively, for the same range of R_0 values.

In Table 5a in the Appendix, the age-specific transmissibility decreases with a younger population, while the age-specific transmission rates after adjusting the contact matrices increase for certain age groups. Specifically, if New York had a younger population structure like Nairobi, the transmission rates among those under 20 years old would increase by 17 %–80 %. Assuming New York's age structure as Los Angeles, the transmission rate among those under 40 years old would grow by 2 %–14 %. If New York adopted Daegu's age structure, the transmission rates among the population aged 40–70 years old would increase by 7 %–18 %. Therefore, the infection rate of COVID-19 might slightly increase or decrease depending on the younger level of susceptible population. However, in all three younger age structures, the infection and deaths among the older population would decrease. These findings highlight the significant role of population age structure and R_0 in shaping the spread of COVID-19 and their varying impacts on different age groups.

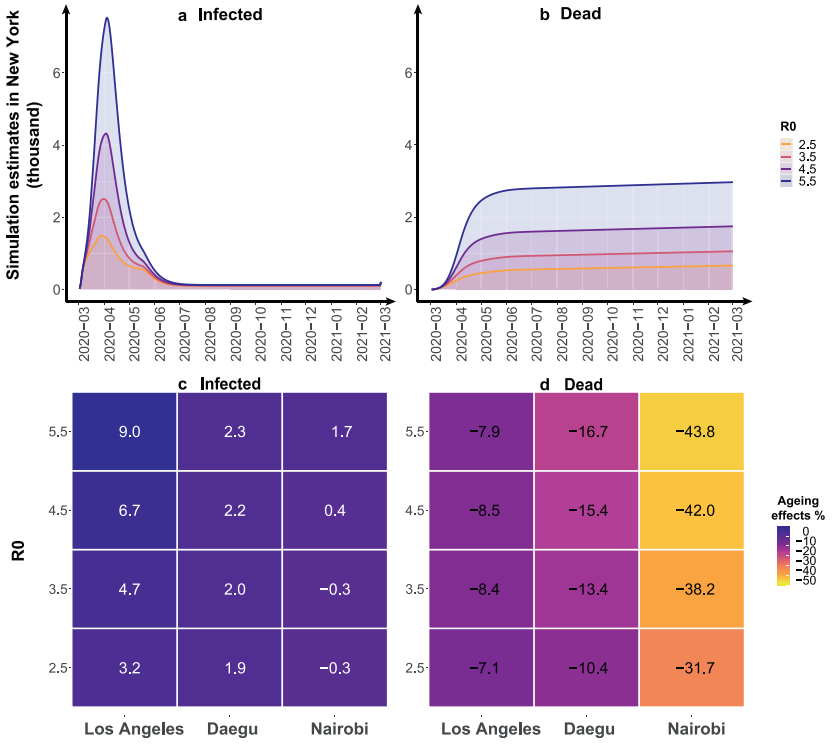

Fig. 8. yThe effects of population age structure on the effectiveness of intervention policy and sensitivity analysis of R_0. Here ageing effects are defined as follows: Ageing effects on infection = $(I_{LA} - I_{NY})/I_{NY}$ and Ageing effects on death = $(D_{LA} - D_{NY})/D_{NY}$.

4. Discussion

COVID-19 has caused an unprecedented public health crisis and economic shock to the global economy. The optimal reopening strategy may vary significantly between cities depending on their demographics and social mixing. We developed, documented, and provided an open-source model which we utilized to examine the effects of different intervention strategies as nations manage risks to different age groups, and as sub-national regions work to curb the spread of COVID-19, and avoid the risks of a second infection wave. We explored the interaction between population age structure and various containment interventions in New York, Los Angeles, Daegu, Nairobi, four cities with different age distributions that were local epicenters of the epidemic from January 2020 to March 2021. We find that not only can social-distancing policies exhibit strong age-differential effects, but that age-targeted interventions can have significant spillovers. Specifically, reduction in the contact rates of population under 20 avoids 14 %, 18 %, 56 % and 99 % infections of all age groups in New York, Los Angeles, Daegu and Nairobi, respectively, which is much more effective than the policy targeting the adults older than 60 years old alone. In particular, to protect the elderly, it is essential to increase social distancing among the younger population, especially those under 20 years old. An older population structure results in a higher fatality risk while might decrease the infection risk. This is particularly critical as colleges and universities, in both cities and small towns, started on-campus activities with students drawn from a globalized pool. A higher basic reproduction number exacerbates the influence of an old population structure on the fatality risk of the elderly. The significant differences in susceptibility and severity by demographic characteristics calls for targeted interventions to suppress the spread of COVID-19.

The study highlights the age-specific effects of various levels of compliance with non-pharmaceutical interventions, indicating that individual interventions alone may not fully curb the infection over a one-year period. However, we observed that a combined strategy of school closure, 50 % working from home, 50 % reduction in other mobility, 10 % quarantine rate, and city lockdown effectively suppresses the pandemic. Our findings reveal that moderate individual social distancing (under 50 %) cannot effectively contain the pandemic, which aligns with some previous studies demonstrating limited effects on reducing infection incidence and prevalence when social distancing is highly effective (Chang et al., 2020; Salje et al., 2020). Moreover, our results show that closing schools can be beneficial for the younger population (under 20), consistent with some previous studies (Rădulescu et al., 2020).

Our study demonstrates the effectiveness of age-targeted policy interventions, which show significant benefits for the entire population. While many policy interventions have primarily focused on the general population or older adults, our simulations reveal that social distancing measures targeting both older and younger populations prove to be the most effective. These interventions also generate spillover effects across other age groups without the need to fully pause the economy. For the middle-aged population, implementing social distancing measures while allowing them to continue working with appropriate protection can be a viable approach. The findings underscore the importance of enforcing social distancing measures among individuals under 20, showing it to be as critical as initiatives aimed at protecting older adults. In contrast, social distancing implemented solely for older populations has limited effectiveness in containing infections. This aligns with prior research on COVID-19 modeling conducted in Ukraine (Kyrychko et al., 2020).

During the early stages of the pandemic, some countries in the US and several other countries opened schools, potentially posing threats not only to the health of the younger population but also endangering the lives of senior adults. An older population age structure exaggerates the fatal impacts of infections, whereas a younger population might result in higher risks of infection due to their higher contact rates compared with the senior adults. Other studies also found that fatality rates were significantly higher among individuals over 80 years old, aligning with the findings in our study (Balabdaoui & Mohr, 2020). Our results demonstrated that maintaining social distancing in the younger population has significant spillover effects on the other age groups of population. A combined social distancing targeting both young (under 20) and the older (older than 60) population significantly improve the effects of each policy intervention. Therefore, the cities with an older population should protect the older people by not only restricting activities of the older population but also confining the activities of the younger ones. These findings align with previous studies suggesting that higher interaction rates among younger populations can lead to increased infections among older individuals (Balabdaoui & Mohr, 2020; Cartocci et al., 2021).

For future pandemics that are similar to COVID-19, some policy guidelines for each city are applicable to facilitate curbing or reopening interventions. The opening-up policies in US resulted in more infected cases (Our World in Data, 2020; Trading Economics, 2020). As schools have already opened, specific policy is needed to warn children and young people to stay social distancing as their exposure to the COVID-19 will be likely to affect the middle-aged and older adults. The Children and COVID-19 data report showed that there were 338.9 thousand of children were tested positive for COVID-19 in the US (American Academy of Pediatrics; & Children's Hospital Association, 2020). It is vital to restrict gatherings and keep social distancing for the young while also protect the old population with community support on essential needs in daily life when vaccines are not available. In addition, there is no strict quarantine and travel restriction in most states of the US, which might result in more domestic import and export cases in the US. It may avoid substantial infection in the Los Angeles and New York if domestic travelers are quarantined for 14 days or a health test that shows the traveler is healthy. The US State Department lifted “Do Not Travel” advisory on August 4, 2020. With more and more countries reopened or reopened with restrictions (US Department of State, 2020), relaxing intervention policies and the lifting travel advisory may impose higher risks to the spread of COVID-19 cases in these nations, especially when vaccination rates were low. Due to economic pressure, Kenya has initiated a subtle reopening policy for businesses, leading to an increase in social activities and mobility among Kenyans. This raised concerns about the potential rise in infection cases and added pressure on the medical system. As higher mobility

among younger population might impose higher risks to older population, thus it becomes even more crucial for Kenya to consider restricting the mobility and social mixing of the younger population to mitigate the risks of further transmission. Daegu also suffered from designing proper reopening strategies. The cluster infection of the nightlife clubs alerted South Korea that it is not the time yet to reopen public gathering establishments. The successfully containing and reopening experience in South Korea might also be good examples for other countries follow or adjust according to the local situation of infection. All the four cities could have curbed the infections at the early stage without spreading the infections across country/city-border. The quarantine intervention is based on the effective testing system and the knowledge of epidemiological survey for the contact tracing. A digital contact tracing tool should be adopted to reduce substantial workload pressure to the medical staff, or the travelers should keep a track on the persons with close contacts each day (Fahey & Hino, 2020; Shahroz et al., 2021). We showed that it was possible to contain the pandemic with strategy of a high quarantine rate (10 %) together with moderate social distancing (50 % reduction in social contacts) and city lockdown (or travel restriction with mandatory self-quarantine), which could largely avoid the costly impacts on the national economy.

Our study has several limitations. One of the key limitations is that our model's social distancing strategy is based on the contact matrices developed at the national level. To distinguish contact matrices at sub-national level, we adjusted the contact matrices according to the population density to the city-specific data. This might introduce uncertainties in the estimates of transmission rates. The population travel data were averaged from monthly or annual traveler statistical database and then we assume the daily importation and exportation were proportional to the daily mobility data from Google mobility reports (Google, 2020), which can introduce uncertainties in the effects of population movement. Therefore, we conducted sensitivity analyses of the population movement on the spread of infection. Second, our model is further constrained by adopting non-localized parameters in each city. This is restricted by incidence data did not tell the age-specific information at a city level, which hindered the possibility to evaluate the age-specific parameters in each city. Since there was no age-specific fatality rate in each city, we adopted the age-specific fatality of China in four cities that was adjusted for censoring demographic information without the consideration of the medical capacity and facility information (Verity et al., 2020). Due to the limited availability of data on the infection rate caused by hospitalized patients at the city level, our model assumes that these patients have limited impacts on the spread of infection. However, it is important to acknowledge that this assumption may not entirely capture the real-life scenario (Barranco & Ventura, 2020). This study applied a unified age-specific fatality rate, which may lead to potential over- or underestimations of death counts across the four cities. Additionally, the model assumes a fixed percent of initial infected cases for each city throughout the simulation, which could introduce uncertainties in the outcomes. Third, there are other environmental factors, such as air pollution, temperature, and humidity, that might have impacts on the transmission rate of COVID-19 geographically (Ma et al., 2020; Shehzad et al., 2021). However, the quantitative effects of these factors remain unclear (Ma et al., 2020; Zhu et al., 2020). Additionally, factors like pandemic preparedness and response strategies can influence COVID-19's health impacts (Lal et al., 2022). Investigating these aspects requires comprehensive healthcare system data, which extends beyond the scope of this study and is thus not explored here. Moreover, it's worth noting that this study primarily focuses on social distancing strategies, and as a result, we did not explore the effects of wearing face masks or vaccination (Reiner et al., 2020). Therefore, while our findings provide valuable insights, it's crucial to interpret them with these limitations in mind and consider further research to enhance the model's accuracy and reliability.

5. Conclusion

In this study, we delve into the age-specific effects of various non-pharmaceutical interventions to gauge their impact on containing the spread of infections in four typical cities. Our findings reveal that implementing social distancing among individuals under 20 not only significantly reduces infection rates within this age group but also creates positive spillover effects that benefit the wider population, particularly in cities with larger elderly populations. This suggests that targeting younger age groups for social distancing could be an effective strategy to protect more vulnerable, older demographics in future pandemics. Additionally, we observed that while younger population structures tend to experience fewer infection-related deaths, they also have higher overall infection rates. This highlights the importance of considering age demographics when designing intervention strategies for infectious diseases. Proactive measures to limit contact among younger populations during early stages of an outbreak could yield substantial health benefits, protecting both younger and older age groups and reducing pressure on healthcare systems. Our study underscores the need for targeted and age-specific intervention policies to enhance public health resilience in the face of future pandemic threats.

CRediT authorship contribution statement

Hao Yin: Writing – review & editing, Writing – original draft, Visualization, Validation, Supervision, Software, Project administration, Methodology, Investigation, Funding acquisition, Formal analysis, Data curation, Conceptualization. **Zhu Liu:** Writing – review & editing, Supervision, Project administration, Methodology, Investigation, Funding acquisition, Conceptualization. **Daniel M. Kammen:** Writing – review & editing, Writing – original draft, Supervision, Resources, Project administration, Methodology, Investigation, Funding acquisition, Conceptualization.

Open access code and data sharing

The COVID-19 incidence data used in this study is extracted from Johns Hopkins University (Johns Hopkins University, 2020), the city-level time-series mobility data were extracted from Google mobility reports (Google, 2020), the contact matrices database is retrieved from Prem et al. (2017), the implemented policy information was collected from government reports and APAPS COVID-19 database (ACAPS, 2020) and the travel data were extracted from multiple sources that are listed in the references. The modeling code and estimation process are available online at https://github.com/HaoYinV/SEIR-HQD and http://rael.berkeley.edu.

Declaration of interests

We declare no competing interests.

Acknowledgements

HY is thankful for funding from the National Natural Science Foundation of China (grant 71904104) and the China Postdoctoral Science Foundation (grant 2019M650726). ZL acknowledges funding from Qiushi Foundation, the Resnick Sustainability Institute at California Institute of Technology and the National Natural Science Foundation of China (grant 71874097 and 41921005). DMK gratefully acknowledges the support of the Zaffaroni Family Foundation, the Karsten Family Foundation, and US NSF CyberSEES Grant 1539585 and NSF InFEWS grant DGE 1633740.

Appendix A. Supplementary data

Supplementary data to this article can be found online at https://doi.org/10.1016/j.idm.2025.03.003.

References

ACAPS. (2020). COVID19 government measures dataset. https://www.acaps.org/covid19-government-measures-dataset.
American Academy of Pediatrics; & Children's Hospital Association. (2020). Children and COVID-19: State data report. https://downloads.aap.org/AAP/PDF/AAPandCHA-ChildrenandCOVID-19StateDataReport7.30.20FINAL.pdf.
Backer, J. A., Klinkenberg, D., & Wallinga, J. (2020). Incubation period of 2019 novel coronavirus (2019-nCoV) infections among travellers from Wuhan, China, 20–28 January 2020. *Eurosurveillance, 25*(5), 2000062.
Balabdaoui, F., & Mohr, D. (2020). Age-stratified discrete compartment model of the COVID-19 epidemic with application to Switzerland. *Scientific Reports, 10*(1), 1–12, 2020.
Banerjee, A., et al. (2020). Estimating excess 1-year mortality associated with the COVID-19 pandemic according to underlying conditions and age: A population-based cohort study. *The Lancet*. https://doi.org/10.1016/S0140-6736(20)30854-0
Barranco, R., & Ventura, F. (2020). Covid-19 and infection in health-care workers: An emerging problem. *Medico-Legal Journal, 88*.
Bayham, J., & Fenichel, E. P. (2020). Impact of school closures for COVID-19 on the US health-care workforce and net mortality: A modelling study. *The Lancet Public Health*. https://doi.org/10.1016/S2468-2667(20)30082-7
BBC. (2020a). Coronavirus: South Korea declares highest alert as infections surge. BBC https://www.bbc.com/news/world-asia-51603251.
BBC. (2020b). Coronavirus: Kenya introduces tight restrictions. BBC https://www.bbc.com/news/world-africa-51917920.
Bi, Q., et al. (2020). Epidemiology and transmission of COVID-19 in 391 cases and 1286 of their close contacts in shenzhen, China: A retrospective cohort study. *The Lancet Infectious Diseases, 20*, 911–919.
Boccia, S., Ricciardi, W., & Ioannidis, J. P. A. (2020). What other countries can learn from Italy during the COVID-19 pandemic. *JAMA Internal Medicine*. https://doi.org/10.1001/jamainternmed.2020.1447
Cao, Z., Zhang, Q., Lu, X., Pfeiffer, D., Wang, L., Song, H., … Zeng, D. D. (2020). *Incorporating human movement data to improve epidemiological estimates for 2019-nCoV. MedRxiv* (pp. 2020–02).
Cartocci, A., Cevenini, G., & Barbini, P. (2021). A compartment modeling approach to reconstruct and analyze gender and age-grouped COVID-19 Italian data for decision-making strategies. *Journal of Biomedical Informatics, 118*, Article 103793.
Centers for Disease Control and Prevention. (2020a). Recommendation regarding the use of cloth face coverings, especially in areas of significant community-based transmission. *CDC website*. https://www.cdc.gov/coronavirus/2019-ncov/prevent-getting-sick/cloth-face-cover.html.
Centers for Disease Control and Prevention. (2020b). Coronavirus disease 2019 - older adults. https://www.cdc.gov/coronavirus/2019-ncov/need-extra-precautions/older-adults.html.
Chang, C. N., Chien, H. Y., & Malagon-Palacios, L. (2022). College reopening and community spread of COVID-19 in the United States. *Public Health, 204*, 70–75.
Chang, S. L., Harding, N., Zachreson, C., Cliff, O. M., & Prokopenko, M. (2020). Modelling transmission and control of the COVID-19 pandemic in Australia. *Nature Communications, 11*.
County of Los Angeles Public Health. (2020). Health officer order's impact on daily life FAQs. http://www.ph.lacounty.gov/media/Coronavirus/docs/HOO/FAQ-SaferatWorkandCommunityOrder.pdf.
Dowd, J. B., et al. (2020). Demographic science aids in understanding the spread and fatality rates of COVID-19. *Proceedings of the National Academy of Sciences of the U S A*. https://doi.org/10.1073/pnas.2004911117
Dyer, O. (2020). Covid-19: US testing ramps up as early response draws harsh criticism. *BMJ*. https://doi.org/10.1136/bmj.m1167
Fahey, R. A., & Hino, A. (2020). COVID-19, digital privacy, and the social limits on data-focused public health responses. *International Journal of Information Management, 55*.
Farrell, T. W., et al. (2020). Rationing limited healthcare resources in the COVID-19 era and beyond: Ethical considerations regarding older adults. *Journal of the American Geriatrics Society, 68*.
Ferguson, N. M., et al. (2020). Impact of non-pharmaceutical interventions (NPIs) to reduce COVID-19 mortality and healthcare demand. *Imperial.Ac.Uk*. https://doi.org/10.25561/77482
Flaxman, S., et al. (2020). *Report 13: Estimating the number of infections and the impact of non-pharmaceutical interventions on COVID-19 in 11 European countries*.
Google. Covid-19 community mobility reports. https://www.google.com/covid19/mobility/, (2020).

Hellewell, J., et al. (2020). Feasibility of controlling COVID-19 outbreaks by isolation of cases and contacts. *Lancet Global Health, 8*, e488–e496.
Hsiang, S., et al. (2020). The effect of large-scale anti-contagion policies on the COVID-19 pandemic. *Nature*. https://doi.org/10.1038/s41586-020-2404-8
Johns Hopkins University. (2020). COVID-19 data repository. https://github.com/CSSEGISandData/COVID-19.
Korea Tourism Organization. (2020). Korea national tourism survey. https://datalab.visitkorea.or.kr/datalab/portal/main/getMainForm.do.
Kyrychko, Y. N., Blyuss, K. B., & Brovchenko, I. (2020). Mathematical modelling of the dynamics and containment of COVID-19 in Ukraine. *Scientific Reports, 10*.
LA County. (2018). *LA county annual report -2017*.
Lal, A., et al. (2022). Pandemic preparedness and response: Exploring the role of universal health coverage within the global health security architecture. *Lancet Global Health, 10*, e1675–e1683.
Leung, K., Wu, J. T., & Leung, G. M. (2021). Effects of adjusting public health, travel, and social measures during the roll-out of COVID-19 vaccination: A modelling study. *The Lancet Public Health, 6*.
Leung, K., Wu, J. T., Liu, D., & Leung, G. M. (2020). First-wave COVID-19 transmissibility and severity in China outside hubei after control measures, and second-wave scenario planning: A modelling impact assessment. *The Lancet*. https://doi.org/10.1016/S0140-6736(20)30746-7
López, L., & Rodó, X. (2020). The end of social confinement and COVID-19 re-emergence risk. *Nature Human Behaviour*. https://doi.org/10.1038/s41562-020-0908-8
Luke, Money, & Rong-Gong, lin II. (2020). L.A. County on verge of becoming COVID-19 epicenter. *LA times*. https://www.latimes.com/california/story/2020-12-18/we-are-getting-crushed-covid-19-ishammering-l-a-countys-healthcare-system-as-deaths-soar-statewide. Last visit date: January 12, 2021.
Ma, Y., et al. (2020). Effects of temperature variation and humidity on the death of COVID-19 in Wuhan, China. *Science of the Total Environment*. https://doi.org/10.1016/j.scitotenv.2020.138226
Mathieu, E., et al. (2020). Coronavirus pandemic (COVID-19). *Our world in data*.
Mersie, A., & Mohammed, O. (2020). Kenya announces phased reopening from coronavirus lockdown. Reuters https://www.reuters.com/article/us-health-coronavirus-kenya-idUSKBN24718R.
Ministry of Health and Welfare. (2020). *Regular briefing of central disaster and safety countermeasure headquarters on COVID-19*. Ministry of Health and Welfare. https://www.mohw.go.kr/eng/nw/nw0101vw.jsp?PAR_MENU_ID=1007&MENU_ID=100701&page=2&CONT_SEQ=353618.
National travel and tourism Office. 2020 U.S. Travel and tourism statistics. https://travel.trade.gov/outreachpages/inbound.general_information.inbound_overview.asp, (2020).
NBC Los Angeles. (2019). *Los Angeles reached record milestone of 50 million visitors in 2018*. NBC News. https://www.nbclosangeles.com/news/local/los-angeles-visitors-2018/2386/.
NYC & company annual report 2020-21, 19. *NY city tourism and Conventions*, (2020) https://indd.adobe.com/view/3e235017-4549-4a3a-af52-171d9b95094e.
Office of the New York State Comptroller, The Tourism Industry in New York City: Reigniting the Return, https://www.osc.ny.gov/reports/osdc/tourism-industry-new-york-city, last visit: September 26, 2021.
Our world in data. *Tourism*, (2020). https://ourworldindata.org/tourism.
Prem, K., Cook, A. R., & Jit, M. (2017). Projecting social contact matrices in 152 countries using contact surveys and demographic data. *PLoS Computational Biology*. https://doi.org/10.1371/journal.pcbi.1005697
Prem, K., et al. (2020a). The effect of control strategies to reduce social mixing on outcomes of the COVID-19 epidemic in wuhan, China: A modelling study. *The Lancet Public Health*. https://doi.org/10.1016/s2468-2667(20)30073-6
Prem, K., et al. (2020b). The effect of control strategies to reduce social mixing on outcomes of the COVID-19 epidemic in wuhan, China: A modelling study. *The Lancet Public Health*. https://doi.org/10.1016/S2468-2667(20)30073-6
Rădulescu, A., Williams, C., & Cavanagh, K. (2020). Management strategies in a SEIR-type model of COVID 19 community spread. *Scientific Reports, 10*.
Reiner, R. C., et al. (2020). Modeling COVID-19 scenarios for the United States. *Nature Medicine, 27*(1 27), 94–105, 2020.
Ryckman, T., et al. (2021). Outbreaks of COVID-19 variants in US prisons: A mathematical modelling analysis of vaccination and reopening policies. *The Lancet Public Health, 6*, e760–e770.
Salje, H., et al. (2020). Estimating the burden of SARS-CoV-2 in France. *Science, 369*, 208–211, 1979.
Santesmasses, D., et al. (2020). COVID-19 is an emergent disease of aging. *Aging Cell, 19*, Article e13230.
Shahroz, M., et al. (2021). COVID-19 digital contact tracing applications and techniques: A review post initial deployments. *Transport Engineer, 5*.
Shehzad, K., Bilgili, F., Koçak, E., Xiaoxing, L., & Ahmad, M. (2021). COVID-19 outbreak, lockdown, and air quality: Fresh insights from New York city. *Environmental Science and Pollution Research, 28*.
The World Bank. (2020). International tourism. https://data.worldbank.org/indicator/ST.INT.ARVL?end=2018&start=1995&view=chart.
Tian, H., et al. (2020). An investigation of transmission control measures during the first 50 days of the COVID-19 epidemic in China. *Science*. https://doi.org/10.1126/science.abb6105
Trading Economics. (2020). Trading economics: Kenya tourist Arrivals. https://tradingeconomics.com/kenya/tourist-arrivals.
US Department of State. (2020). *International Travel*. https://travel.state.gov/content/travel/en/international-travel.html.
Vahia, I. V., et al. (2020). COVID-19, mental health and aging: A need for new knowledge to bridge science and service. *American Journal of Geriatric Psychiatry*. https://doi.org/10.1016/j.jagp.2020.03.007
Verity, R., et al. (2020). Estimates of the severity of coronavirus disease 2019 : A model-based analysis. *The Lancet Infectious Diseases*. https://doi.org/10.1016/S1473-3099(20)30243-7
Verity, R, Okell, LC, Dorigatti, I, Winskill, P, Whittaker, C, Imai, N, … Dighe, A (2020). Estimates of the severity of coronavirus disease 2019: a model-based analysis. *The Lancet Infectious Diseases, 20*(6), 669–677.
Wallinga, J., & Teunis, P. (2004). Different epidemic curves for severe acute respiratory syndrome reveal similar impacts of control measures. *American Journal of Epidemiology*. https://doi.org/10.1093/aje/kwh255
Wu, J. T., Leung, K., & Leung, G. M. (2020). Nowcasting and forecasting the potential domestic and international spread of the 2019-nCoV outbreak originating in wuhan, China: A modelling study. *The Lancet*. https://doi.org/10.1016/S0140-6736(20)30260-9
Zhu, Y., Xie, J., Huang, F., & Cao, L. (2020). Association between short-term exposure to air pollution and COVID-19 infection: Evidence from China. *Science of the Total Environment*. https://doi.org/10.1016/j.scitotenv.2020.138704